JACC: CARDIOVASCULAR IMAGING VOL. 7, NO. 5, 2014

ISSN 1936-878X/$36.00
PUBLISHED BY ELSEVIER INC. http://dx.doi.org/10.1016/j.jcmg.2013.11.010

ORIGINAL RESEARCH

Molecular and Cellular Correlates of Cardiac Function in End-Stage DCM

A Study Using Speckle Tracking Echocardiography

Andrea M. Cordero-Reyes, MD, Keith Youker, PhD, Jerry D. Estep, MD, Guillermo Torre-Amione, MD, PhD, Sherif F. Nagueh, MD

Houston, Texas

OBJECTIVES We sought to compare the effects of interstitial fibrosis and myocardial force generation/relaxation elements on left ventricular (LV) function in patients with end-stage dilated cardiomyopathy (DCM).

BACKGROUND Interstitial fibrosis is common in patients with advanced heart failure. However, the extent to which it affects cardiac function remains unclear.

METHODS Longitudinal, radial, and circumferential strain; strain rate during systole (SR_S) and strain rate during early diastole (SR_E); LV volume; LV ejection fraction; mean pulmonary capillary wedge pressure (PCWP); and e′ were measured in 20 DCM patients. Myocyte diameter, interstitial fibrosis, messenger ribonucleic acid (mRNA) levels of molecules implicated in fibrosis and function (transforming growth factor beta, titin [TTN] N2B and N2BA isoforms, collagen type I, collagen type III, sarcoplasmic reticulum Ca^{2+}-ATPase [SERCA2a], phospholamban [PLB], and protein levels of SERCA2a, phosphorylated PLB, and Smad2/3) were correlated with strain from 4 regions per patient (LV apex, midlateral, septum, and right ventricular free wall) as well as LV global function. In another group of 8 DCM patients, we evaluated LV structure and function before and after LV assist device.

RESULTS Significant correlations were present among ejection fraction, e′ velocity, PCWP, LV end-diastolic volume/PCWP ratio, strain, SR_S, SR_E, and mRNA expression of TTN N2B, N2BA, SERCA2a, PLB, and protein levels of SERCA2a and phosphorylated PLB ($r = 0.53$ to 0.95, $p < 0.05$). Weak to no associations were present between strain and interstitial fibrosis and its molecular determinants. In patients with repeat studies, regional strain and SR_E best tracked the changes in mRNA expression of TTN isoform N2BA and mRNA and protein expression of SERCA2a.

CONCLUSIONS LV systolic and diastolic functions in DCM are primarily associated with myocardial force generation/relaxation elements. (J Am Coll Cardiol Img 2014;7:441–52) © 2014 by the American College of Cardiology Foundation

From the Methodist DeBakey Heart and Vascular Center, The Methodist Hospital, Houston, Texas. The authors have reported that they have no relationships relevant to the contents of this paper to disclose.

Manuscript received September 26, 2013; revised manuscript received November 14, 2013, accepted November 15, 2013.

JACC: CARDIOVASCULAR IMAGING, VOL. 7, NO. 5, 2014
MAY 2014:441–52

Interstitial fibrosis is a common finding in patients with dilated cardiomyopathy (DCM) and can play an important role in affecting left ventricular (LV) function in these patients (1,2). However, a recent study has not shown a significant association between replacement fibrosis (as assessed by cardiac magnetic resonance) in DCM patients and LV diastolic function (3). Of note, the study did not evaluate interstitial fibrosis and did not examine cardiac mechanics (3). We therefore sought to evaluate the effects of interstitial fibrosis on cardiac function in DCM patients and determine the extent to which its effects on cardiac function dominate over those of sarcomeric and sarcoplasmic proteins. We obtained cardiac tissue to measure fibrosis in addition to molecules that determine the development of fibrosis such as transforming growth factor beta-1 (TGFβ1) and its downstream mediators: phosphorylated Smad2/3 (1). Given the effects of calcium cycling proteins and titin (TTN) on LV systolic and diastolic function, we selected these molecules to determine their contributions in these patients. For calcium-cycling proteins, several studies have shown a significant relation between the protein levels of sarcoplasmic reticulum Ca^{2+}-ATPase (SERCA2a), sarcoplasmic reticulum calcium uptake, and the force frequency relationship in patients with heart failure (4,5). For TTN isoforms, a number of previous reports showed the important role that this molecule plays in determining LV diastolic stiffness (6). These relationships are of potential clinical interest, as changes in the level of these proteins or their phosphorylation status can be used to improve LV function in patients with end-stage heart failure.

ABBREVIATIONS AND ACRONYMS

ANOVA = analysis of variance

COLIA1 = collagen type I

COLIIIA1 = collagen type III

DCM = dilated cardiomyopathy

EF = ejection fraction

GAPDH = glyceraldehyde-3-phosphate dehydrogenase

LV = left ventricular

LVAD = left ventricular assist device

mRNA = messenger ribonucleic acid

PCWP = pulmonary capillary wedge pressure

PLB = phospholamban

RV = right ventricular

SERCA2a = sarcoplasmic reticulum Ca^{2+}-ATPase

SR = strain rate

SR_A = strain rate during late diastole

SR_E = strain rate during early diastole

SR_{IVR} = strain rate during the isovolumic relaxation period

SR_S = strain rate during systole

TGF = transforming growth factor

TTN = titin

METHODS

Patient population. The study sample included 20 heart failure patients with DCM who underwent cardiac transplantation in the previous 2 years. The patients were on contemporary medical therapy for systolic heart failure including cardiac resynchronization therapy in 13 patients. Clinical, echocardiographic, and invasive hemodynamic evaluations were performed within 20 to 60 days of transplantation. Full-thickness specimens of the LV apex, midseptum, and midlateral walls were removed from explanted hearts as well as the right ventricular (RV) free wall at the time of transplantation. Cardiac tissue was obtained from the hearts of 4 donors without cardiac disease who died of head injuries or bleeding (mean age 32 ± 8 years; LV ejection fraction [EF] 60 ± 4%).

To help evaluate the underlying mechanisms behind the change in cardiac function, we sought to compare the changes in cardiac pathology and messenger ribonucleic acid (mRNA) and protein expression with the changes in cardiac function in a setting that leads to reverse remodeling. To achieve this objective, we included 8 patients with a wide duration range of left ventricular assist device (LVAD) support who had the device implanted as a bridge to cardiac transplantation. These 8 patients had cardiac imaging on 2 occasions: just before LVAD implantation and just before cardiac transplantation. The duration of LVAD support varied from 32 to 1,402 days. Changes in segmental function of the distal 1-cm region of the lateral wall were related to tissue analysis results.

Echocardiographic imaging. A complete echocardiographic study was performed according to standard views (parasternal and apical views) and guidelines (7–9). Care was taken to obtain 3 parasternal circular short-axis tomograms: basal (identified by the mitral valve), papillary, and apical (no papillary muscles noted) levels. Two-dimensional image acquisition was carried out at a frame rate of 40 to 50 frames/s, and 3 cardiac cycles were stored in cine loop format. The study was stored digitally for offline analysis.

Echocardiographic analysis. Echocardiographic measurements were performed by an observer without knowledge of histopathology and molecular findings. LV volumes, EF, left atrial volume, and Doppler velocities and ratios were measured per American Society of Echocardiography guidelines (7,8). Deformation analysis was performed using a commercially available system (syngo Velocity Vector Imaging, Siemens Healthcare, Malvern, Pennsylvania) (10). Adequate tracking was verified in real time and corrected, if necessary. Longitudinal strain and strain rates (SR) (strain rate during systole [SR_S], strain rate during early diastole [SR_E], and strain rate during late diastole [SR_A]) were measured from the apical views. Circumferential strain and radial strain (and SR) were measured from the short-axis views (9). Global SR during the isovolumic relaxation period (SR_{IVR}) and SR_E were measured, and the ratios of E/SR_{IVR} and E/SR_E were derived (9). Mean interobserver difference for the different strain and SR measurements varied from −3.0% to 2.5% (SD: 0.5% to 2.0%). Mean intraobserver difference ranged from −2%

to 2% (SD: 0.6% to 1.5%). Apical untwisting velocity was measured and used for analysis of the molecular and cellular determinants of untwisting at that level. The segmentation used is the standard segmentation with the following segments: basal, mid, and distal anterior wall; basal, mid, and distal inferior wall; basal, mid, and distal lateral wall; basal, mid, and distal septum; base and midposterior (or inferolateral) wall; LV apex; and RV free wall (9). This same segmentation was used for molecular and histopathological analysis.

Myocardial tissue analysis. Tissue was procured under an approved institutional review board protocol. Tissue samples were cut from each region into 3 adjacent portions: 2 were immediately snap-frozen and used for polymerase chain reaction and protein studies, and 1 portion was fixed in 2% paraformaldehyde, processed, paraffin-embedded, and cut into 5-μm sections. To measure fibrosis, sections were stained with Masson's trichrome stain (Sigma-Aldrich, St. Louis, Missouri). The slides were then cover-slipped and analyzed at 20× magnification using an Olympus AX70 microscope (Olympus Corporation, Tokyo, Japan). Five representative pictures were taken from each slide and analyzed for fibrosis using Image Pro Plus version 4.0 analysis software (Media Cybernetics, Silver Spring, Maryland). A color cube–based selection criterion was used to denote positive staining, and stained/unstained areas were measured. The results expressed are the average percentage of tissue area (pixels) stained by the blue dye. Analysis was performed by an observer blinded to the sample identities. Myocyte diameter was measured at the level of the nucleus in hematoxylin-eosin–stained sections. At 20× magnification fields, a point-to-point perpendicular line drawn across the cross-sectional area of the myocytes at the level of the nucleus and the diameter length was measured with the computer imaging software. A total of 50 myocytes/slide were measured from each tissue specimen, and the mean ± SD per section were noted (11).

Analysis of gene expression. Total mRNA was isolated from cardiac tissues using ribonucleic acid (RNA)-binding columns (RNaqueous-4-polymerase chain reaction, Ambion, Life Technologies, Grand Island, New York). RNA was immediately reverse-transcribed into complementary deoxyribonucleic acid with a kit using random primers (iScript, Bio-Rad, Hercules, California) according to the manufacturers' directions. Real-time reaction mixtures contained 11 μl of H_2O, 12 μl of IQ SYBR Green Supermix (Bio-Rad), 1 μl of primers, and 1 μl of complementary deoxyribonucleic acid template (25 μl total). Sense and antisense primers were chosen from the RTPrimerDB public primer database for humans. Reactions were aliquoted into 96-well plates and plates were sealed, centrifuged at 500 *g* for 60 s, and amplified for 40 cycles of 10 s at 95°C, 30 s at 55°C, and 10 s at 72°C. Real-time polymerase chain reactions were analyzed in a MyIQ5 iCycler (Bio-Rad) in triplicate and normalized to glyceraldehyde-3-phosphate dehydrogenase (GAPDH), a housekeeping gene run on the same plate for every sample that was tested (12). This approach was performed to normalize for potential differences in the amount of RNA in different regions. Gene expression levels were determined for TGFβ1, TTN isoforms N2B and N2BA (13), collagen type I (COLIA1), collagen type III (COLIIIA1), sarcoplasmic reticulum Ca^{2+}-ATPase (SERCA2a), and phospholamban (PLB).

Protein expression analysis. Cardiac tissue was placed in 10 times its volume of tissue lysis buffer (Invitrogen, Carlsbad, California) with added protease inhibitor cocktail (Sigma-Aldrich). Samples were then homogenized and incubated on ice for 20 min with gentle vortex every 5 min. Samples were centrifuged at 10,000 *g* at 4°C for 15 min, and the pellet was discarded and the supernatant was quantified for protein using a photometer. Samples were standardized and solubilized in Laemmli buffer with B-mercaptoethanol and placed in 80°C water for 5 min. Twenty-five micrograms of each sample were blotted on a nylon membrane using an immune-blot apparatus and antibody stained. Antibody staining was initiated with blocking for 30 min in a blocking buffer (phosphate-buffered saline with 1% horse serum), incubation with primary antibody diluted in blocking buffer for 1 h and washed. Blots were then incubated for 1 h in secondary antibody conjugated with alkaline phosphatase diluted in blocking buffer, followed by washing with phosphate-buffered saline. The final step for color development used was NBT/BCIP (Thermo Scientific, Waltham, Massachusetts) as a substrate for 15 to 20 min. Staining intensity was measured by densitometric analysis with the Image Pro Plus software. Protein expression levels were determined for SERCA2a, phosphorylated PLB, and phosphorylated Smad2/3 (all antibodies from Santa Cruz Biotechnology, Santa Cruz, California).

Statistics. Data are presented as mean ± SD or median (25th to 75th percentile) where appropriate. Repeated-measures analysis of variance (ANOVA) and 1-way ANOVA on ranks were used to compare the structural and functional parameters between the different segments in patients. Subsequent

JACC: CARDIOVASCULAR IMAGING, VOL. 7, NO. 5, 2014
MAY 2014:441–52

pairwise multiple comparison procedures were performed using the Dunn or Holm-Sidak method. Patients and control subjects were compared using an unpaired Student *t* test or rank sum test based on data distribution. Regression analysis (linear and nonlinear) was used to relate the extent of collagen, myocyte size, and gene/protein expression to systolic and diastolic function (1 region/patient and thus using patients as the units of analysis). Measurement variability was determined by repeated measurements from 6 studies at 2 time points 3 weeks apart. The absolute difference was calculated as well as the mean ± SD. A p value <0.05 was used to define statistical significance.

RESULTS

The group (20 patients; 8 women) had a mean age of 53 ± 13 years. All patients had advanced heart failure with a New York Heart Association functional class III to IV. RV function was severely depressed in 4 patients, moderately depressed in 8 patients, and mildly depressed in 2 patients, and the rest had normal RV function. Moderate mitral regurgitation was present in 3 patients, and the rest had trace to mild lesions. Moderate tricuspid regurgitation was present in 1 patient, another patient had severe regurgitation, and the rest had trace to mild lesions. The echocardiographic and hemodynamic findings are summarized in Table 1.

Table 1. Summary of Echocardiographic and Hemodynamic Measurements

Heart rate, beats/min	80.0 ± 3.0
Systolic blood pressure, mm Hg	106.0 ± 4.0
Diastolic blood pressure, mm Hg	64.0 ± 3.0
Pulmonary artery systolic pressure, mm Hg	50.0 ± 5.0
Pulmonary artery diastolic pressure, mm Hg	29.0 ± 3.0
Mean right atrial pressure, mm Hg	13.0 ± 1.4
Mean pulmonary capillary wedge pressure, mm Hg	21.0 ± 2.0
Cardiac index, l/min/m^2	1.9 ± 0.1
Left ventricular end-diastolic volume index, ml/m^2	111.0 ± 9.0
Left ventricular end-systolic volume index, ml/m^2	82.0 ± 10.0
Ejection fraction, %	30.0 ± 3.5
Left atrial maximal volume index, ml/m^2	47.0 ± 4.0
Mitral E/A ratio	2.4 ± 0.4
Deceleration time of mitral E velocity, ms	151.0 ± 18.0
Average e′ velocity, cm/s	5.7 ± 0.5
Average E/e′ ratio	16.0 ± 2.0
Average a′ velocity, cm/s	5.6 ± 0.9
Peak O_2 consumption, ml/kg/min	9.3 ± 1.5

Values are mean ± SD.

Interstitial fibrosis and myocyte size. Table 2 presents a summary of the findings for the 4 regions. Significant differences were noted for the percentage of fibrosis between mid-RV free wall and LV segments ($p < 0.05$ vs. all 3 LV regions). Likewise, myocyte diameter was smaller for RV myocytes versus LV myocytes, albeit with some overlap ($p < 0.05$ vs. LV midlateral wall) (Fig. 1).

mRNA levels of selected molecules involved in myocardial dysfunction and interstitial fibrosis in patients and comparison with normal control subjects. There was evidence of up-regulation of mRNA levels of several genes when patients were compared with control subjects: TGFβ1, TTN N2BA isoform (non-normal distribution), COLIA1, COLIIIA1, and PLB (all p values <0.01). However, mRNA levels of SERCA2a were lower in patients compared with control subjects ($p < 0.01$).

Regional variations were present for the mRNA levels of COLIA1, COLIIIA1, and TGF-β. TGF-β and COLIA1 mRNA levels among different LV regions were significantly correlated (using individual patients as the units of analysis: $r = 0.45$ to 0.8, $p < 0.05$).

Protein expression. SERCA2a protein levels were significantly lower in patients versus control subjects ($p < 0.01$). However, phosphorylated PLB and phosphorylated Smad2/3 protein levels were significantly higher in patients versus control subjects (both $p < 0.05$).

The regional protein expression of SERCA2a was similar to its gene expression, with a significant relationship noted in the 4 sampled regions ($r = 0.48$ to 0.63, $p < 0.05$). Regional protein expression of phosphorylated PLB was related to its gene expression with a significant relationship noted in the 4 sampled regions ($r = 0.74$ to 0.88, $p < 0.01$). Similarly, phosphorylated Smad2/3 and TGFβ1 gene expression were significantly correlated ($r = 0.85$ to 0.94, $p < 0.01$).

Myocyte size and interstitial fibrosis and segmental function. Systolic and diastolic functions were depressed in the apex, lateral, septal, and RV lateral wall segments, as reflected by the reduced longitudinal, radial, and circumferential strain, SR_S and SR_E (Table 2). Significant associations between SR_S and strain, as well as SR_E, and each of strain and SR_S were observed for all 4 regions ($r = 0.6$ to 0.94, $p < 0.05$).

An inverse relationship between the extent of interstitial fibrosis and segmental systolic function was present but it did not reach the statistical significance level (the best relationship was present for apical longitudinal SR_S with $r = 0.47$, $p = 0.09$).

Table 2. Histopathology and Myocardial Strain/SR_S and SR_E in the Left and Right Ventricle

	LV Apex	Midlateral	Midseptum	RV Free Wall
Fibrosis, %	26.0 ± 5.6	26.7 ± 4.8	30 ± 5.5	10.0 ± 2.0*
Myocyte diameter, μm	68.0 ± 3.9	76.0 ± 3.8	66.0 ± 3.0	61.0 ± 2.7†
Longitudinal strain, %	−4.3 (−5.6 to −2.8)†	−6.0 (−9.2 to −4.2)	−3.0 (−4.8 to −1.5)†	−5.6 (−7.6 to −2.8)
Longitudinal SR_E, s^{-1}	0.10 (0.06 to 0.14)†	0.19 (0.13 to 0.29)	0.10 (0.05 to 0.19)†	0.16 (0.08 to 0.26)
Circumferential strain, %	−4.2 (−6.2 to −1.45)†	−7.5 (−10.4 to −4.4)	−4.4 (−6.8 to −2.1)†	−3.5 (−4.8 to −1.75)†
Circumferential SR_E, s^{-1}	0.1 (0.06 to 0.17)†	0.18 (0.10 to 0.24)	0.12 (0.08 to 0.17)†	0.12 (0.04 to 0.18)†
Radial strain, %	11.4 (7.3 to 21.5)†	21.0 (10.3 to 30.6)	10.6 (4.2 to 17.0)†	13.3 (7.2 to 23.0)†
Radial SR_E, s^{-1}	−0.29 (−0.7 to −0.14)†	−0.8 (−1.4 to −0.46)	−0.37 (−0.75 to −0.15)†	−0.32 (−0.89 to −0.27)†

Values are mean ± SD or median (25th to 75th percentile). *$p < 0.05$ versus 3 other groups. †$p < 0.05$ versus midlateral wall.
LV = left ventricular; RV = right ventricular; SR_E = strain rate during early diastole; SR_S = strain rate during systole.

However, significant correlations were observed between myocyte diameter and strain, SR_S, and SR_E (for longitudinal and circumferential strain and SR_S [$r = 0.52$ to 0.76], for longitudinal and circumferential SR_E [$r = -0.65$ to -0.78, $p < 0.05$], all p values <0.05) (Fig. 2) such that segments with a larger myocyte diameter had less deformation.

mRNA expression of COLIA1, COLIIIA1, TGFβ1, and phosphorylated Smad and segmental function. No significant associations were noted between strain and SR_S measurements and mRNA expression of TGFβ1, COLIA1, COLIIIA1, and phosphorylated Smad2/3.

Similarly, there were no significant correlations with SR_E except for septal longitudinal SR_E in which weak associations were noted with mRNA expression of COLIA1 and phosphorylated Smad2/3 ($r = -0.45$ to 0.5, $p = 0.05$).

mRNA and protein expression of SERCA2a and PLB and segmental function. Strain and SR_S were related to mRNA expression of SERCA2a, SERCA2a/PLB ratio, and protein expression of SERCA2a and

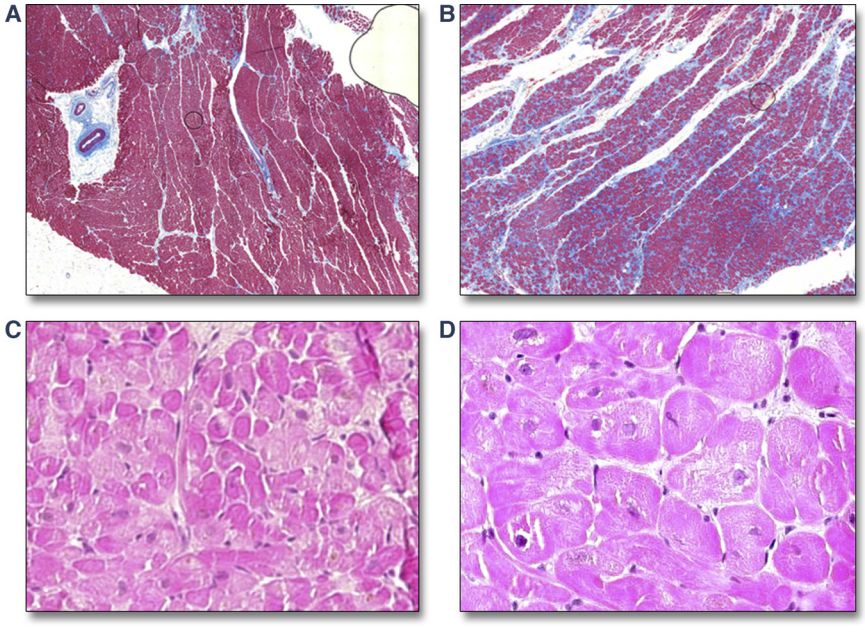

Figure 1. Fibrosis Deposition With Trichrome Stain and Myocyte Size From a Hematoxylin and Eosin Stain

(A) Lower amount of deposition in the right ventricular free wall of patient A. **(B)** Increased fibrosis in the left ventricular free wall in the same patient. Myocyte size in patient A is also smaller in the right ventricular free wall **(C)** than in the left ventricular free wall **(D)**. Magnification ×20.

phosphorylated PLB. More deformation was noted in segments with higher SERCA2a (mRNA and protein) content (apex, r = 0.5 for radial strain to −0.83 for longitudinal strain; lateral wall, r = −0.55 for circumferential SR_S to −0.82 for longitudinal strain; septum, r = −0.53 for longitudinal strain to −0.6 for circumferential strain; RV, r = −0.56 to −0.65; all p values <0.05) (Fig. 3).

Diastolic function was also better for segments with higher SERCA2a (mRNA and protein) content and higher phosphorylated PLB protein content (apex, r = 0.5 to 0.65; lateral wall, r = 0.55 to 0.61; septum, r = 0.5 to 0.68; RV, r = 0.52 to 0.66; all p values <0.05). The results were largely unchanged when the ratio of the molecules to GAPDH was used (for systolic parameters, r = −0.5 to −0.84; for diastolic parameters, r = 0.53 to 0.73; all p values <0.05).

mRNA expression of TTN N2B and N2BA and segmental function. Strong correlations were observed between circumferential and longitudinal SR_E and mRNA expression of TTN N2B and N2BA isoforms and their ratio (apex, r = 0.65 to −0.93; lateral, r = 0.78 to −0.87; septal, r = 0.63 to −0.67; RV, r = 0.62 to −0.71; all p values <0.05) (Fig. 4). The results remained significant when the ratio of TTN mRNA molecules to GAPDH was used (r = 0.79 to 0.94; all p values <0.05).

mRNA and protein expression and LV global function. To examine the determinants of global LV function, the average values of mRNA expression and protein expression in the 3 LV regions were used. LV volumes and EF were not related to interstitial fibrosis or its molecular determinants. However, they were related to myocyte diameter such that larger ventricles (both end-diastolic and -systolic volumes) and lower EF were associated with larger myocytes (end-diastolic volume, r = 0.56; end-systolic volume, 0.64; EF, −0.79; p < 0.05). Likewise, significant associations were present between global longitudinal strain and each of the following: myocyte size, interstitial fibrosis, and mRNA SERCA2a/PLB ratio (r = −0.58 to 0.73; all p values <0.05).

For LV diastolic function, we examined the determinants of relaxation and stiffness. For relaxation, the mRNA and protein expression levels of SERCA2A related well to average early diastolic annular velocity (e′), SR_{IVR}, and SR_E (Fig. 5). For stiffness, the ratio of mRNA expression of TTN N2BA to N2B isoforms decreased from grade I to grade III diastolic dysfunction (ANOVA, p = 0.013) and was related to E/e′, E/SR_{IVR}, and E/SR_E (r = −0.6 to 0.68, p < 0.05) as well as LV EDV/pulmonary capillary wedge pressure (PCWP) ratio (r = 0.68, p < 0.05).

In comparison, there was no significant relationship between the different parameters of LV global diastolic function and fibrosis (best relationship noted was between mean PCWP and mRNA expression of COLIA1 [r = 0.41, p = 0.11]).

Determinants of apical untwisting velocity. Apical untwisting velocity was related to the twisting velocity (r = 0.7, p < 0.05). Aside from this relationship, the strongest significant determinant of the untwisting velocity was the mRNA expression level of TTN N2B (Fig. 6).

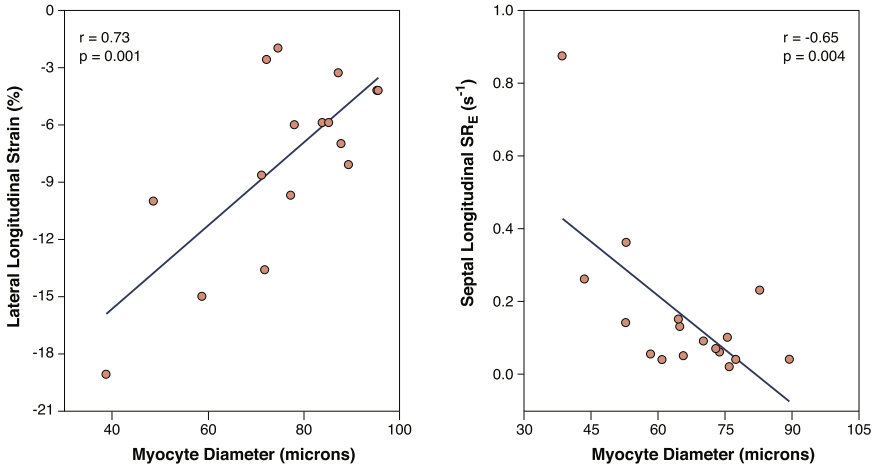

Figure 2. Myocyte Diameter and Segmental Strain and Early Diastolic Strain Rate From 2 Left Ventricular Regions

Relationship between myocyte diameter and longitudinal strain for lateral wall segments to the **left** and longitudinal septal SR_E to the **right** (linear regression). SR_E = strain rate during early diastole.

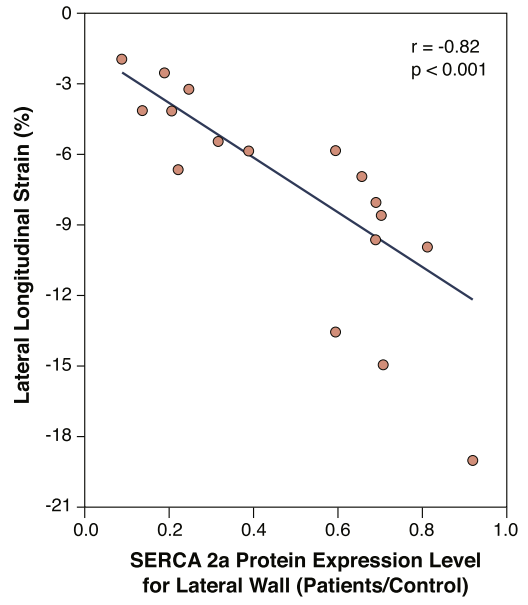

Figure 3. SERCA2a Protein Expression Level and Lateral Longitudinal Strain

Relationship between SERCA2a protein expression level (DCM/control) and lateral longitudinal strain (linear regression). DCM = dilated cardiomyopathy; SERCA2a = sarcoplasmic reticulum Ca^{2+}-ATPase.

Cardiac function, mRNA, and protein expression before and after LVAD support. With LVAD support, the group of 8 patients (48 ± 11 years of age; 2 females) showed a significant decrease in LV and left atrial volumes, with an increase in LVEF ($p < 0.05$), but smaller changes in global strain parameters (Table 3). Overall, improvement was noted in segmental strain and SR_E (Table 4). The percentage of changes was used in the analysis so each patient would serve as his or her control.

There was a wide range of changes in cardiac pathology and mRNA and protein changes in the 8 patients. The magnitude and direction of changes in mRNA and protein levels of SERCA2a were similar ($r = 0.78$, $p = 0.02$). Likewise the changes in mRNA and protein levels of PLB were correlated ($r = 0.8$, $p = 0.02$). Although mRNA levels of COLIA1 and COLIIIA1 decreased, the change in fibrosis and myocyte diameter did not reach the significance level.

With respect to the structure-function relationship, there were no significant correlations between changes in fibrosis and myocyte size and changes in segmental systolic and diastolic function ($r = 0.1$ to 0.2, all p values >0.6). In comparison, the changes in mRNA and protein levels of SERCA2a related well with the changes in longitudinal ($r = 0.73$, $p = 0.03$) and circumferential strain (Fig. 7) such that the increase in SERCA2a protein levels was accompanied by more longitudinal and circumferential compression (more negative strain). For radial strain, the association was of borderline significance ($p = 0.08$). Longitudinal and circumferential SR_E appeared to track the changes in mRNA expression

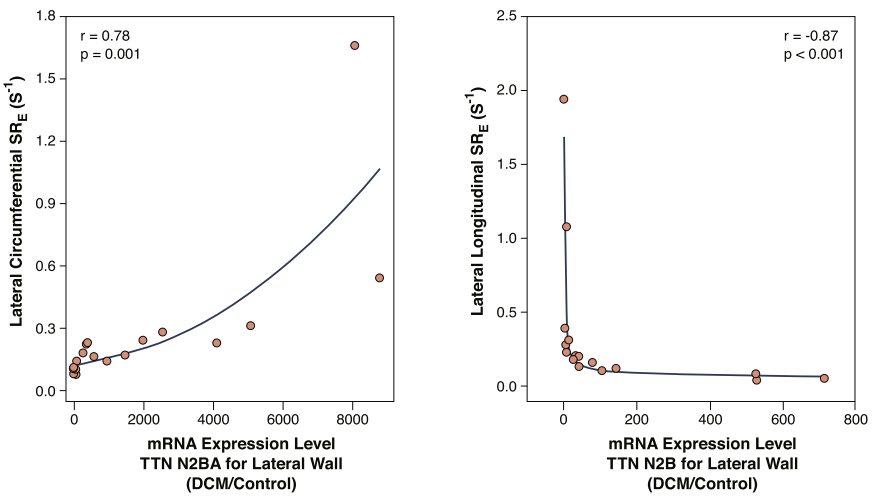

Figure 4. TTN N2B and N2BA mRNA Expression Level and Lateral Wall Early Diastolic Strain Rate

(Left) Relationship between mRNA expression level of TTN N2BA (DCM/control) in lateral wall segments (quadratic equation of $y = y_0 + ax + bx^2$) and lateral circumferential SR_E. **(Right)** Relationship between mRNA expression level of TTN N2B (DCM/control) and lateral longitudinal SR_E (inverse first-order equation of $y = y_0 + a/x$). mRNA = messenger ribonucleic acid; TTN = titin; other abbreviations as in Figures 2 and 3.

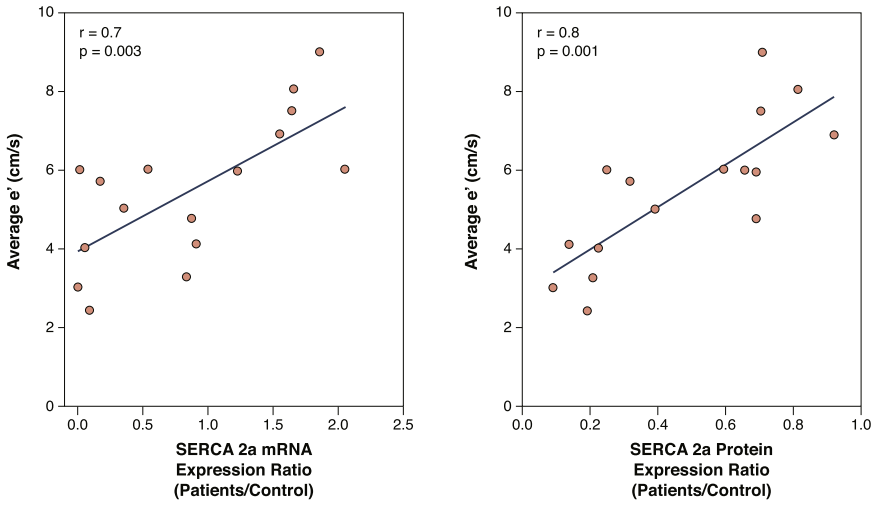

Figure 5. SERCA2a mRNA Expression, Protein Expression, and Average e' Velocity

Relationship between mRNA expression level of SERCA2a and average e′ **(left)** and between SERCA2a protein expression level (DCM/control) and average e′ (linear regression) **(right)**. For 3 patients, e′ was not entered in the regression analysis due to merging of e′ and a′. Abbreviations as in Figures 3 and 4.

of TTN N2BA such that patients with higher gene expression levels of the isoform had an increase in SR_E after LVAD support compared with baseline (Fig. 7). The changes in radial SR_E did not reach the significance level ($p = 0.09$).

DISCUSSION

The results of the current study lend credence to the notion that a strong predictor of the abnormal cardiac function in patients with DCM lies with cellular expression of calcium-cycling proteins and TTN isoforms, although the study cannot prove a cause-and-effect relationship given its design. The results were consistent on both the segmental and global levels. Furthermore, the results were very similar whether one considers conventional or more novel indexes of cardiac function. The results with respect to interstitial fibrosis were weaker in this population and somewhat different from other diseases in which replacement fibrosis is common as in

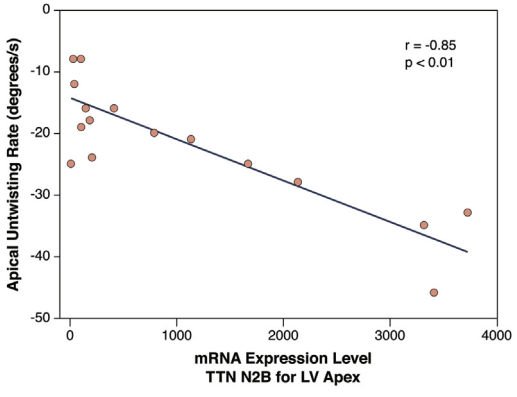

Figure 6. TTN N2B mRNA Expression Level and Apical Untwisting Rate

Relationship between apical untwisting rate and apical mRNA expression level of TTN N2B (linear regression). LV = left ventricular; other abbreviations as in Figure 4.

Table 3. Global Cardiac Function Before LVAD Implantation and Before Cardiac Transplantation

	Before LVAD Implantation	Before Cardiac Transplantation
Heart rate, beats/min	91.0 ± 14.0	80.0 ± 9.0
Systolic blood pressure, mm Hg	98.0 ± 13.0	90.0 ± 9.0
LV end-diastolic volume, ml	320.0 ± 48.0	178.0 ± 51.0*
LV end-systolic volume, ml	259.0 ± 43.0	135.0 ± 51.0*
LVEF, %	20.0 ± 2.0	34.0 ± 6.0*
LA maximal volume index, ml	101.0 ± 15.0	57.0 ± 12.0*
Global longitudinal strain, %	−4.6 ± 2.0	−5.7 ± 1.0
Global SR_{IVR}, s^{-1}	0.06 ± 0.40	0.10 ± 0.05*
Global SR_E, s^{-1}	0.23 ± 0.12	0.35 ± 0.20†

Values are mean ± SD. *$p < 0.05$. †$p = 0.06$.
LA = left atrial; LVAD = left ventricular assist device; LVEF = left ventricular ejection fraction; SR_{IVR} = strain rate during the isovolumic relaxation period; other abbreviations as in Table 2.

Table 4. Segmental Function Before LVAD Implantation and Before Cardiac Transplantation

	Before LVAD Implantation	Before Cardiac Transplantation
Longitudinal strain, %	−2.8 ± 0.8	−5.6 ± 1.3*
Longitudinal SR_E, s^{-1}	0.21 ± 0.16	0.43 ± 0.29*
Circumferential strain, %	−4.7 ± 3.0	−6.5 ± 4.0
Circumferential SR_E, s^{-1}	0.39 ± 0.40	0.59 ± 0.30*
Radial strain, %	11.5 ± 14.0	17.0 ± 13.0†
Radial SR_E, s^{-1}	−0.56 ± 0.40	−0.82 ± 0.40*

Values are mean ± SD. *$p < 0.05$. †$p = 0.08$.
Abbreviations as in Tables 2 and 3.

post-infarction cardiomyopathy, and its extent can be used to determine the presence of myocardial viability (14–16).

Relationship of myocardial structure to function. Although, in general, larger amounts of interstitial fibrosis are associated with worse function, the nature and severity of the disease may account for the different observations in this study. The extent and pattern of fibrosis in DCM are known to be different from those seen in patients with coronary artery disease and post-infarction cardiomyopathy in which there are large areas of replacement fibrosis. Interestingly, cellular hypertrophy was associated with a worse segmental function (systolic and diastolic). This observation is similar to previous studies (11), and it is likely that cellular hypertrophy occurs as a compensatory response to segmental dysfunction and fibrosis. Furthermore, interstitial abnormalities may contribute to the wasted contraction and LV dysfunction in these patients, and it is difficult to isolate these mechanisms of interaction by imaging.

Collagen, TGF-β, and myocardial function. The presence of collagen, its isoforms, and the status of collagen cross-linking all play an important role in determining myocardial stiffness. Likewise, TGF-β1, through its downstream mediator phosphorylated Smad2/3, results in increased matrix production and reduced collagen degradation and thus increased interstitial fibrosis (1,17). Although the relationship between fibrosis and cardiac function in this group of patients was weaker than other patient groups, trends were noted with some segmental strain parameters as well as mean PCWP. Furthermore, fibrosis was significantly related to LV global longitudinal strain.

The study of the evolution of cardiac structural and functional changes is better done in animals. This would allow serial measurements and the determination of which abnormality occurs earliest and which best tracks the changes in cardiac function. However, there can be limitations to this approach as large animal models differ from and may not necessarily have the human pathology. For example, canine models of pacing-induced heart failure, which results in DCM, do not show myocyte hypertrophy and fibrosis. On the other hand, large animal models with coronary microembolization show the characteristic findings noted in humans with ischemic cardiomyopathy including fibrosis and hypertrophy but also microinfarctions, which are absent in most patients with isolated DCM (18).

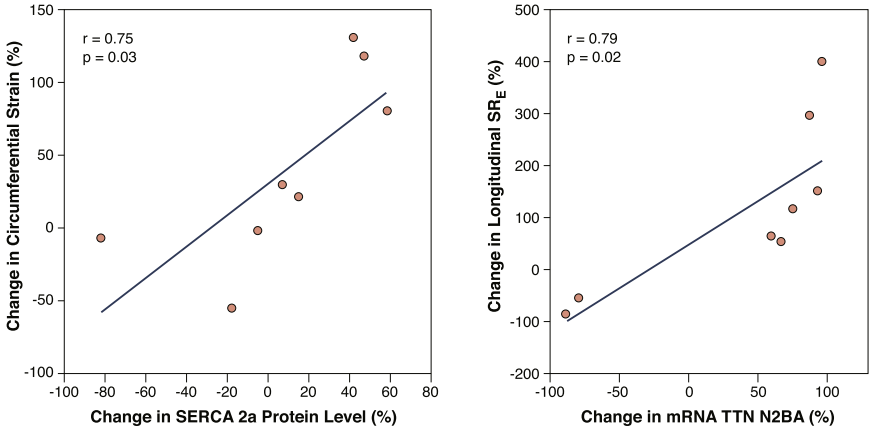

Figure 7. Changes in SERCA2a Protein Expression, TTN N2BA mRNA Expression With LVAD and Myocardial Function

(Left) Relationship between the change in SERCA2a protein level (post-/pre-LVAD) versus the change in circumferential strain (pre-/post-LVAD). **(Right)** Relationship between the change mRNA expression level of TTN N2BA and the change in longitudinal SR_E (post-/pre-LVAD). LVAD = left ventricular assist device; other abbreviations as in Figures 2 to 4.

TTN isoform expression and myocardial function. The macromolecule TTN is expressed in 2 isoforms that affect myocardial stiffness. The 2 forms are N2B, with a shorter extensible segment compared with the N2BA isoform, which has longer segments. The relative expression of the 2 isoforms has been shown to relate to myocardial and chamber stiffness in several diseases including patients with systolic and diastolic heart failure (13,19–21). A higher amount of N2B isoform is accompanied by increased myocardial stiffness, whereas greater N2BA isoform expression can lead to a more complaint ventricle. In that regard, previous animal studies have shown an inverse relationship between segmental SR_E and the regional stiffness constant measured invasively (16). Accordingly, the significant correlations between SR_E and N2B (negative correlation) and N2BA (positive correlation) are consistent with the effects of isoform switching on LV stiffness. Likewise, the relationship of LV filling pattern, LV stiffness surrogate, and the ratio of mRNA expression of TTN N2BA to N2B are consistent with the findings at the segmental level and the previously referenced studies in humans.

We noted a significant association between the mRNA expression of TTN N2B and apical untwisting rate. Previous work in an animal model with pacing-induced tachycardia showed increased expression of the more compliant N2BA isoform in the subendocardium of animals with systolic dysfunction and reduced restoring forces (22). To our knowledge, this is the first study in humans to show the strong association between the less extensible TTN N2B isoform and apical untwisting, such that higher mRNA levels of this molecule were accompanied by a higher untwisting rate. The stronger restoring forces of TTN N2B (vs. TTN N2BA) leading to faster untwisting likely provide the mechanistic link for this observation.

SERCA2a, PLB, and myocardial strain. Calcium transport by the sarcoplasmic reticulum plays a major role in the regulation of myocyte contractility and relaxation. In that regard, SERCA2a pump activity is 1 of the important mechanisms that leads to lower calcium concentration in the sarcoplasm and thus results in muscle relaxation. Cardiac SERCA2a activity is regulated by PLB. Dephosphorylated PLB acts as an inhibitor of SERCA2a, whereas phosphorylation of the PLB molecule relieves SERCA2a of the inhibitory effects and results in increased calcium transport across the sarcoplasmic reticulum (23). Our findings of significant associations between segmental strain, global LV systolic and diastolic function, and the mRNA and protein expression of SERCA2a, SERCA2a/PLB ratio, and phosphorylated PLB are in line with the cited studies and support the important role of these molecules in determining cardiac function in patients with end-stage DCM.

Study limitations. The results presented are based on data gathered from patients with advanced cardiac disease. Whether similar relationships occur in less symptomatic patients is an important question to address. However, it is challenging to acquire full-thickness biopsy specimens from multiple LV regions in patients with earlier stages of cardiac disease. There was a time lapse between imaging and obtaining cardiac tissue in the initial group of 20 patients. Therefore, we cannot exclude that further changes in cardiac pathology could have occurred between the 2 time points.

We sought to study the changes in cardiac pathology and mRNA and protein expression. This is ideally done by looking at changes in the same patient over a number of time points. However, it is difficult to obtain repeat LV samples from the same patient. Accordingly, we acquired cardiac tissue at 2 time points from each patient and obtained a wide range of pathology changes as the patients had a wide range of LVAD support duration. The control group was younger than the patient group, but this was unavoidable as young individuals are usually the ones selected for donor hearts.

Other potentially important molecules were not examined. We sought to evaluate the ones that have been well characterized and known to affect interstitial fibrosis and myocyte function. Although we did not evaluate the protein levels or phosphorylation state of TTN isoforms, which are known to alter myocardial stiffness (24), our results already strongly support the important role that this molecule plays in determining regional and global LV diastolic function. The small sample size may have precluded us from showing significant correlations between fibrosis and a number of cardiac function parameters. Nevertheless, the statistical analysis suggests that the effects of fibrosis on cardiac function are weaker in this patient group than what have been reported in other patients.

The frame rate may have led to underestimation of peak SR measurements. However, we believe that this is a homogeneous effect that applies to all acquisitions and is unlikely to have a differential effect on the results. Invasive measurements of LV stiffness constant were not performed, and surrogate noninvasive and invasive parameters were obtained instead. However, the use of noninvasive

imaging is unlikely to have led to different results because the same surrogate of stiffness was related to the parameters of interest, namely, fibrosis and mRNA and protein expression levels of key molecules that determine cellular function. If the noninvasive parameters were a poor surrogate of tissue stiffness, one would have seen weak correlations across the board rather than only with fibrosis.

CONCLUSIONS

The results of this study support the ongoing efforts in identifying novel approaches to the treatment of patients with LV systolic dysfunction. Importantly, increasing the expression of SERCA2a appears to have a promising role in the treatment of patients with advanced heart failure (25). Furthermore, given the strong association between TTN isoforms and indexes of LV regional and global diastolic function, LV diastolic performance can be improved in these patients by increased phosphorylation of TTN by protein kinase G as well as increasing cyclic guanosine monophosphate levels (24).

Reprint requests and correspondence: Dr. Sherif F. Nagueh, Methodist DeBakey Heart and Vascular Center, 6550 Fannin, SM-677, Houston, Texas 77030. *E-mail: snagueh@houstonmethodist.com.*

REFERENCES

1. Manabe I, Shindo T, Nagai R. Gene expression in fibroblasts and fibrosis involvement in cardiac hypertrophy. Circ Res 2002;91:1103–13.
2. Moreo A, Ambrosio G, De Chiara B, et al. Influence of myocardial fibrosis on left ventricular diastolic function: noninvasive assessment by cardiac magnetic resonance and echo. Circ Cardiovasc Imaging 2009;2:437–43.
3. Malaty AN, Shah DJ, Abdelkarim AR, Nagueh SF. Relation of replacement fibrosis to left ventricular diastolic function in patients with dilated cardiomyopathy. J Am Soc Echocardiogr 2011;24:333–8.
4. Hasenfuss G, Reinecke H, Studer R, et al. Relation between myocardial function and expression of sarcoplasmic reticulum Ca(2+)-ATPase in failing and nonfailing human myocardium. Circ Res 1994;75:434–42.
5. Heerdt PM, Holmes JW, Cai B, et al. Chronic unloading by left ventricular assist device reverses contractile dysfunction and alters gene expression in end-stage heart failure. Circulation 2000;102:2713–9.
6. LeWinter MM, Granzier H. Cardiac titin; a multifunctional giant. Circulation 2010;121:2137–45.
7. Lang RM, Bierig M, Devereux RB, et al. Recommendations for chamber quantification: a report from the American Society of Echocardiography's Guidelines and Standards Committee and the Chamber Quantification Writing Group, developed in conjunction with the European Association of Echocardiography, a branch of the European Society of Cardiology. J Am Soc Echocardiogr 2005;18:1440–63.
8. Nagueh SF, Appleton CP, Gillebert TC, et al. Recommendations for the evaluation of left ventricular diastolic function by echocardiography. J Am Soc Echocardiogr 2009;22:107–33.
9. Mor-Avi V, Lang RM, Badano LP, et al. Current and evolving echocardiographic techniques for the quantitative evaluation of cardiac mechanics: ASE/EAE consensus statement on methodology and indications endorsed by the Japanese Society of Echocardiography. J Am Soc Echocardiogr 2011;24:277–313.
10. Pirat B, Khoury DS, Hartley CJ, et al. A novel feature-tracking echocardiographic method for the quantitation of regional myocardial function: validation in an animal model of ischemia-reperfusion. J Am Coll Cardiol 2008;51:651–9.
11. Thohan V, Stetson SJ, Nagueh SF, et al. Cellular and hemodynamics responses of failing myocardium to continuous flow mechanical circulatory support using the DeBakey-Noon left ventricular assist device: a comparative analysis with pulsatile-type devices. J Heart Lung Transplant 2005;24:566–75.
12. Pattyn F, Speleman F, De Paepe A, Vandesompele J. RTPrimerDB: the real-time PCR primer and probe database. Nucleic Acids Res 2003;31:122–3.
13. Makarenko I, Opitz CA, Leake MC, et al. Passive stiffness changes caused by upregulation of compliant titin isoforms in human dilated cardiomyopathy hearts. Circ Res 2004;95:708–16.
14. Zhang Y, Chan AK, Yu CM, et al. Strain rate imaging differentiates transmural from non-transmural myocardial infarction: a validation study using delayed-enhancement magnetic resonance imaging. J Am Coll Cardiol 2005;46:864–71.
15. Chan J, Hanekom L, Wong C, Leano R, Cho GY, Marwick TH. Differentiation of subendocardial and transmural infarction using two-dimensional strain rate imaging to assess short-axis and long-axis myocardial function. J Am Coll Cardiol 2006;48:2026–33.
16. Park TH, Nagueh SF, Khoury DS, et al. Impact of myocardial structure and function postinfarction on diastolic strain measurements: implications for assessment of myocardial viability. Am J Physiol Heart Circ Physiol 2006;290:H724–31.
17. Lamberts RR, Willemsen MJ, Perez NG, Sipkema P, Westerhof N. Acute and specific collagen type I degradation increases diastolic and developed tension in perfused rat papillary muscle. Am J Physiol Heart Circ Physiol 2004;286:H889–94.
18. Houser SR, Margulies KB, Murphy AM, et al. Animal models of heart failure: a scientific statement from the American Heart Association. Circ Res 2012;111:131–50.
19. Neagoe C, Kulke M, del Monte F, et al. Titin isoform switch in ischaemic human heart disease. Circulation 2002;106:1333–41.
20. Nagueh SF, Shah G, Wu Y, et al. Altered titin expression, myocardial stiffness, and left ventricular function in patients with dilated cardiomyopathy. Circulation 2004;110:155–62.
21. Borbély A, van der Velden J, Papp Z, et al. Cardiomyocyte stiffness in

diastolic heart failure. Circulation 2005;111:774–81.

22. Bell SP, Nyland L, Tischler MD, McNabb M, Granzier H, LeWinter MM. Alterations in the determinants of diastolic suction during pacing tachycardia. Circ Res 2000; 87:235–40.

23. Periasamy M, Bhupathy P, Babu GJ. Regulation of sarcoplasmic reticulum Ca^{2+} ATPase pump expression and its relevance to cardiac muscle physiology and pathology. Cardiovasc Res 2008; 77:265–73.

24. van Heerebeek L, Franssen CP, Hamdani N, Verheugt FW, Somsen GA, Paulus WJ. Molecular and cellular basis for diastolic dysfunction. Curr Heart Fail Rep 2012;9: 293–302.

25. Jessup M, Greenberg B, Mancini D, et al., Calcium Upregulation by Percutaneous Administration of Gene Therapy in Cardiac Disease (CUPID) Investigators. Calcium Upregulation by Percutaneous Administration of Gene Therapy in Cardiac Disease (CUPID): a phase 2 trial of intracoronary gene therapy of sarcoplasmic reticulum Ca2+-ATPase in patients with advanced heart failure. Circulation 2011;124:304–13.

Key Words: cardiomyopathy ■ diastole ■ echocardiography ■ molecular ■ strain.